Comparison of Horizontal and Vertical Scintillometer Crosswinds during Strong Foehn with Lidar and Aircraft Measurements

MARKUS FURGER

Paul Scherrer Institut, Labor für Atmosphärenchemie, Villigen, Switzerland

PHILIPPE DROBINSKI

Laboratoire de Météorologie Dynamique, Ecole Polytechnique, Palaiseau, France

ANDRÉ S. H. PRÉVÔT, RUDOLF O. WEBER, WERNER K. GRABER

Paul Scherrer Institut, Labor für Atmosphärenchemie, Villigen, Switzerland

BRUNO NEININGER

MetAir AG, Illnau, Switzerland

(Manuscript received 11 January 2001, in final form 12 June 2001)

ABSTRACT

Measurements of the horizontal and vertical wind component by a crosswind scintillometer during foehn, the chinooklike downslope windstorm in the Alps, are presented. Because of the sparsity of vertical velocity measurements in the immediate vicinity, the scintillometer calibration is checked mainly with horizontal wind measurements. Then it is assumed that the calibration is the same for both components. The concept was tested during the Mesoscale Alpine Programme field campaign in the autumn of 1999, during which two scintillometers were deployed. Strong, long-lasting, quasi-stationary downward motions on the order of 5 m s^{-1} and horizontal wind speeds of over 30 m s^{-1} were detected during strong foehn phases within the valley. Aircraft measurements of various transects near the light paths are compared with two crosswind evaluation techniques. One of them, the slope method, tends to overestimate the actual wind speed by about 20%, whereas the peak technique gives values that are about 10% too low for high wind speeds. The peak method also fails to measure meaningful vertical crosswind speeds. The scintillometer data of one particular foehn storm are compared with nearby Doppler lidar data. The agreement of the horizontal measurements is reasonable. Discrepancies are attributed to topographic and dynamic effects that cause significant spatial inhomogeneities in the wind field. The applicability of continuous scintillometer vertical crosswind measurements in mountainous terrain is demonstrated.

1. Introduction

The vertical component *w* of the three-dimensional wind vector is an important quantity in meteorology. However, measuring this quantity reliably has been difficult with conventional instruments because of small average vertical velocities close to the ground. Measurements at higher altitudes are best done with remote sensing techniques, because in situ measurements (pilot balloons, constant level balloons, and aircraft) are only available for short episodes, may be inaccurate or not representative because of the turbulent fluctuations, or are expensive. Continuous vertical wind measurements at elevated layers have become available only recently with the introduction of Doppler remote sensing techniques, such as acoustic or electromagnetic radars (sodars, radar wind profilers, and lidars).

An alternative method suggested here is using crosswind scintillometers. Such instruments were developed to measure the component of the wind field perpendicular to the optical path between the scintillometer transmitter and the receiver (Lawrence et al. 1972). The measurement represents a weighted average of the wind speed over the full pathlength, with winds near the center of the path getting a larger weight. Typical scintillometers consist of a transmitter with a light source (laser or incoherent infrared diode) and a receiver with two sensors that measure the intensity of the incoming light as a function of time. The measured wind component lies in the plane defined by the transmitter diode and the two receiver sensors. A cross-covariance anal-

Corresponding author address: Dr. Markus Furger, Paul Scherrer Institut, Labor für Atmosphärenchemie, CH-5232 Villigen PSI, Switzerland.
E-mail: markus.furger@psi.ch

ysis of the two signals yields the crosswind speed (Wang et al. 1981). Because over flat terrain the horizontal wind component is significantly larger than the vertical component, the sensors are usually arranged horizontally and adjacent to each other to yield the horizontal crosswind speed. If rotated 90°, the same receiver could be used for measuring the vertical wind component (Hill et al. 1991). We developed this concept further and constructed scintillometers with three sensors arranged in the shape of the letter ''L'' (Poggio et al. 2000). Thus we can measure simultaneously the vertical and the horizontal components of the wind field. This approach proves especially useful when applied in mountainous terrain, where terrain-following flows exhibit substantial mean vertical velocities. The concept has been applied to relatively weak, thermally induced valley flow with wind speeds up to 10 m s^{-1} during the Vertical Ozone Transport in the Alps Mesolcina Valley Campaign in 1996 (Furger et al. 2000; Poggio et al. 2000). Nonzero vertical winds were observed relatively close to the sloping valley floor near the end of the valley but not 400 and 600 m above the more level valley floor in the lower part of the valley. Apart from these results, Poggio (1998) did not discuss vertical crosswind measurements further.

This study pursues primarily the goal of validating the horizontal and vertical crosswind speed measurements during a severe downslope windstorm, when significant wave activity and turbulence occurs in mountainous terrain (Brinkmann 1971; Hoinka 1985; Seibert 1990). Under such conditions, unusually strong vertical components show up in the measurements. An estimate of the accuracy of the vertical crosswind velocity measurement is prerequisite for further use of the data, for example, for calculations of turbulent kinetic energy or momentum fluxes.

The observed high crosswind velocities led to some debate within the scientific community about the plausibility of the scintillometer measurements. A careful analysis of the scintillometer calibration was needed to establish the validity of the measurements over the full range of observations. We discuss the scintillometers' performance and calibration by comparison with other, independent measurements and by analyzing the performance of two common crosswind evaluation techniques. The data were collected during an international field campaign in the Alps in the autumn of 1999. Independent measurements at the exact location were unfortunately too sparse for a thorough statistical analysis, but for the available data good agreement was found.

We will put special emphasis on the novelty of continuous, path-averaged, highly time-resolved vertical velocity measurements in a valley atmosphere. Because vertical wind measurements in the vicinity of the scintillometers were collected by aircraft only, we will also look at horizontal wind components measured by aircraft and lidar to validate our crosswind measurements. We describe the technical aspects of the scintillometer and its calibration in section 2 and the experiment setup and methods for data analysis in section 3. A critical discussion of the plausibility of our measurements is given in section 4.

FIG. 1. Receiver of PSI's scintillometer showing the three-mirror configuration for the simultaneous measurement of horizontal and vertical crosswind.

2. Instrumentation

a. Paul Scherrer Institute scintillometer

1) HARDWARE

The scintillometers built at the Paul Scherrer Institute (PSI) follow the design described in Wang et al. (1978; 1981). The instruments are of the large-aperture type to prevent scintillation saturation effects. Each instrument consists of a transmitter and a receiver. The transmitter contains a 15-cm protected gold-coated spherical mirror that is illuminated by a pulsed infrared diode. The gold coating enhances reflectivity to 96% in the infrared wavelengths between 750 and 1500 nm. The receiver contains three 15-cm protected aluminum-coated spherical mirrors arranged in an L shape, as shown in Fig. 1. The incoming light is detected with a photodiode, amplified, and bandpass filtered. A second amplifier further enhances the signal, and additional filtering conditions the signal for analog-to-digital conversion. Thus, signal conditioning is done by the hardware in the receiver, and all signal analysis is subsequently performed by software. Analysis techniques have been described by Wang et al. (1981) and were further evaluated in Poggio et al. (2000). Technical specifications of the scintillometer are given in Table 1. The standard deviations

TABLE 1. Technical characteristics of PSI's scintillometers.

Technical details	
Mirror diameter*	0.15 m
Mirror focal length*	0.30 m
Light source	Pulsed infrared diode
Peak wavelength	890 nm
No. of mirrors	Transmitter: 1 Receiver: 3 (for vertical and horizontal crosswind components)
Measurement details	
Recorded parameters	Std dev of light intensity
Measurement range	0–40 m s^{-1}
Accuracy	12% (0.25 m s^{-1} for weak wind speeds)
Precision	0.25 m s^{-1}
Sampling rate	0.15 Hz (1 measurement every 7 s)

* For both transmitter and receiver.

of the light-intensity fluctuations of each sensor are stored together with the crosswind speeds and the maxima of the covariance functions. They can be used as an indicator of the quality of the crosswind measurements in cases of low light intensity due to haze, clouds, or rain. Our scintillometers were experimentally calibrated for 10-min-averaged horizontal crosswind speeds from 0 to 10 m s^{-1}.

The measurements described here were sampled in 7-s intervals. A measurement cycle consisted of 1 s of light-intensity measurements at 2 kHz (three channels). Data processing on a ''notebook'' computer with a 100-MHz 80486-DX processor took approximately 6 s. The sampling rate of 2 kHz allows us to measure wind speeds of up to 40 m s^{-1} (Poggio 1998).

2) REMARKS ON SCINTILLOMETER CALIBRATION

Scintillometer crosswind calibration comprises different sources of error, for example, variations of wind speed and the refractive index structure parameter C_n^2 along the path; violations of Taylor's hypothesis (Willis and Deardorff 1976), which would cause a decorrelation of the detected signals; or changes in the turbulence spectrum, which may lead to effects similar to saturation of scintillation (see below). Crosswind evaluation techniques work differently under different atmospheric conditions (Wang et al. 1981; Poggio 1998). We used the slope method described there, which relates the slope of the covariance function at zero time delay to the crosswind speed. The slope method is insensitive to wind fluctuations but very sensitive to C_n^2 inhomogeneities along the light path. The peak method relates the time delay of the peak of the covariance function to the crosswind speed. We compared slope and peak method with each other and with aircraft measurements taken close to the light paths to gain information on the performance of the two techniques under different wind conditions.

Information on measurement accuracy is given in Table 1. All of our scintillometers were calibrated identically for horizontal and vertical components. Calibration of a scintillometer has to be done empirically by comparison with a standard wind-measuring technique (Poggio et al. 2000). This works well for the horizontal component but less so for the vertical component, because most calibration experiments have to be performed over flat terrain, where the light path is within reach of other wind sensors distributed along the light path. Close to the ground, vertical velocities are small, and many conventional instruments are inaccurate because of their low-speed threshold. We argue that horizontal and vertical velocity calibration are the same, and that we can thus use a horizontal calibration experiment to calibrate the vertical component. The underlying assumption is that turbulence is homogeneous (e.g., Lee and Harp 1969). In addition, the validity of Taylor's frozen turbulence hypothesis is assumed. For the case study presented here we show (section 3c) that these conditions hold, because we consider a situation with a strong downslope windstorm (well-developed foehn), and such flows tend to be turbulent over a large vertical extent.

Strong turbulence might result in scintillation saturation (Clifford et al. 1974), which results in an underestimation of the crosswind speed. To see whether saturation may be of concern to us, we searched information on C_n^2 in the literature. Doviak and Zrnić (1993) present vertical profiles of C_n^2 for the troposphere that indicate that this parameter is generally less than 10^{-14} $m^{-2/3}$ at levels high above ground. Near the ground, that is, in the surface layer, the values may grow larger than 10^{-14} $m^{-2/3}$ (Kohsiek 1985; Drobinski et al. 1999; Hill et al. 1980), depending on the season. Poggio (1998) has estimated that C_n^2 values smaller than 10^{-14} $m^{-2/3}$ will not lead to saturation for our scintillometer configuration and pathlength. Thus, we do not expect saturation effects to occur in our Rhine Valley setup.

Foehn flows may also exhibit substantial wave activity in the lower layers, especially during the foehn buildup phase. As a consequence, spatially separated instruments may reveal systematic differences in their measurements due to these waves, depending on their respective position within the wave. During such situations, the homogeneity assumption for the wind field will be invalid. Foehn flows often become supercritical or jetlike in favorable areas (Pettré 1982) and hence are completely different from the weaker, thermally induced valley circulations. These complicating factors have to be borne in mind when discussing the intercomparison results.

b. Lidar

The French transportable wind lidar (TWL), a scanning Doppler lidar operated by the Laboratoire de Météorologie Dynamique (Drobinski et al. 1998, 2001), was located in Vilters, Switzerland (Fig. 2). It scanned the atmosphere by sweeping the azimuth angle from

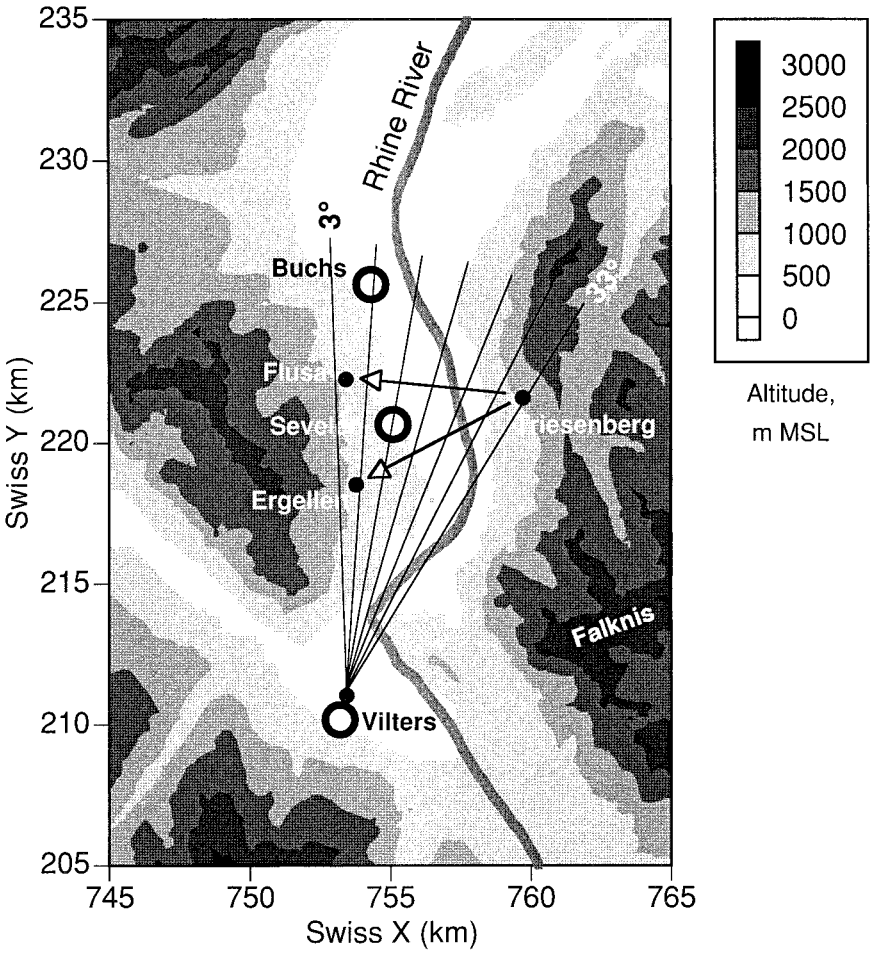

FIG. 2. Map of the experimental setup in the Rhine Valley, the FORM target area. Sevelen is located at 47°07′N and 09°29′E. Black circles denote the villages mentioned in the text; arrows indicate scintillometer light beams. Thin black lines denote the TWL lidar beams used in the analysis. The scintillometer transmitters were located in Triesenberg; the receivers were located in Flusa and Ergellen.

262° to 142°, with an increment of 5°, and the elevation from 4° to 28°, with an increment of 2°. It used an accumulation of 10 shots (i.e., 5 s) to retrieve one radial velocity profile along the TWL line of sight, with an accuracy of 0.5 m s^{-1}. This scanning mode produced velocity estimates between portions of spherical surfaces along the valley axes and bounded laterally by the sidewalls. The radial velocity profiles were retrieved by using Doppler frequency estimators and a quality control procedure (Dabas et al. 1999), with a negative sign indicating flow toward the lidar. The maximum range depends on the aerosol content of the atmosphere. The horizontal maximum range is 5–10 km during foehn events, when the air is clean, and is greater than 10 km without foehn. Range resolution is 200 m along the beam. The processing bandwidth allowed for radial velocity measurements in the range of ± 50 m s^{-1}. For this study, we extracted data from a circular arc over seven adjacent directions spanning a geographic azimuth angle of 30° from 3° to 33° at an elevation of 4° (Fig. 2).

c. Aircraft

The Dimona aircraft of MetAir AG is a light aircraft (motorglider) equipped with chemical and meteorological sensors placed in two wing pods and the fuselage (Neininger et al. 2001). The aircraft cruising speed ranges from 40 to 55 m s^{-1}. Sampling rates for meteorological parameters vary between 10 and 0.1 Hz. The data used here have been integrated to 1- or 60-s intervals. The movement and orientation in the earth-fixed system was measured by an advanced global positioning system receiver, which also measures the attitude angles of the aircraft (update rate 5 Hz, accuracy better than 0.5°), and an accelerometer to improve the resolution of the vertical component. The flow relative to the aircraft was captured by differential pressure sensors (a

five-hole probe in front of one of the underwing pods, where the acceleration also was measured). The three-dimensional wind is the vector difference between the two. The usual accuracy is 0.5 m s^{-1} per wind component, for each individual measurement at 10 Hz. This cannot be improved much by averaging, because the main contribution, especially for the vertical, is an unknown systematic error. Under adverse conditions (turns, change of satellites, etc.) the accuracy may be reduced.

3. Measurements and methods

a. Experimental setup

We demonstrate the scintillometer's wind-measuring capabilities with data obtained during the Foehn-in-the-Rhine-Valley-during-MAP (FORM) subproject of the Mesoscale Alpine Programme (MAP) field experiment in the European Alps in 1999 (Bougeault et al. 2001). This experiment produced an unusually dense dataset (in space and time) that is well suited for comparisons of various instruments.

Two scintillometers were in operation across the Rhine Valley (Fig. 2). Pathlengths were 6.5 and 6.2 km, with the path centers at about 500 m above ground level. The transmitters were installed in Triesenberg, Liechtenstein. According to the names of the farms on which the receivers were placed, the northern light beam will be referred to as Flusa and the southern beam will be referred to as Ergellen. Both scintillometers were calibrated identically, but they measured at different locations, with the centers of the light beams being some 2 km apart. The data analyzed here were collected from 20 to 24 October 1999, with special emphasis on the last day. On that day, a strong foehn occurred that removed the cold air from the whole valley. In the evening, foehn breakdown was caused by an advancing cold front. The transportable wind lidar was located in Vilters, about 10 km south (upstream) of Sevelen, Switzerland. The distance of the scintillometers from the lidar ranged from 7 to 13 km. The lidar beam passed within 0–400 m above the scintillometer light paths.

Because MetAir's Dimona aircraft was not flying at the height of the light beams on 24 October, we included data from 20–22 October 1999. On those days a total of 14 aircraft transects were flown at altitudes within 100 m from the light beams. On four transects, wind speeds in excess of 15 m s^{-1} were measured. We extracted data from flight sections within less than ±200-m horizontal distance from the position of the light path centers, covering six to eight measurements per transect. These data were compared with simultaneous, 1-min-averaged scintillometer measurements. The accuracy of each scintillometer had been determined to be 12.5% for 10-min averages (Poggio et al. 2000).

TABLE 2. Test for the validity of Taylor's hypothesis for the Ergellen scintillometer. The condition is fulfilled if the standard deviation σ (column 3) is smaller than one-half the mean value of the horizontal crosswind component (column 4). Boldface values indicate where this criterion is violated.

	Horizontal crosswind			
Time (UTC)	No. of cases	V	σ	Abs(V/2)
0000	506	5.7	2.07	2.9
0100	506	9.1	2.35	4.5
0200	506	12.6	2.70	6.3
0300	507	19.8	2.94	9.9
0400	506	20.2	3.66	10.1
0500	507	18.3	3.64	9.1
0600	506	27.4	7.51	13.7
0700	506	32.9	5.27	16.4
0800	507	31.3	4.64	15.6
0900	506	34.0	3.46	17.0
1000	507	35.7	4.11	17.8
1100	507	29.3	3.89	14.6
1200	506	27.9	4.88	14.0
1300	506	25.3	4.50	12.6
1400	506	29.0	5.06	14.5
1500	507	22.5	5.09	11.3
1600	506	18.6	3.91	9.3
1700	506	1.0	8.40	**0.5**
1800	506	−7.9	3.45	3.9
1900	506	−6.1	2.81	3.0
2000	506	−4.3	3.05	**2.2**
2100	506	−5.0	3.46	**2.5**
2200	506	−5.7	2.90	2.9
2300	506	−0.7	2.17	**0.4**

b. Power spectra

Turbulence information was obtained from power spectra for both the horizontal and vertical wind components at Flusa and Ergellen. The spectra were computed from the time series sampled with equidistant time steps of 7 s (raw data). Their power spectral density $S(f)$ was calculated by a standard nonparametric technique (Press et al. 1989). For this purpose, the time series was divided into K equally long segments of length $M = 2048$, overlapping by one-half of their length. For each segment, the periodogram was obtained by applying a Welch filter and using a fast Fourier transform. The periodograms of all segments were averaged, in this way reducing the sampling error of the spectral estimate by a factor of about $9K/11$. The power spectral density was normalized such that the total power is contained in the positive frequencies.

c. Validity of Taylor's hypothesis

The validity of Taylor's hypothesis [section 2a(2)] can be tested by comparing the standard deviation of the horizontal crosswind speed with the mean value. Willis and Deardorff (1976) give $\sigma < 0.5\ V$ as an estimator, σ being the standard deviation and V the mean value of the horizontal crosswind component. We computed σ and V for 1-h intervals. Table 2 shows that this cri-

terion was fulfilled during the foehn phase in Ergellen. Flusa (not shown) exhibited a similar behavior.

4. Discussion

Empirical calibrations of instruments require one or several other instruments measuring the same physical quantity. During MAP–FORM, no monitoring instrument was actually collocated with the scintillometer light paths, but the transportable wind lidar measured at times in an inclined plane that contained the Ergellen receiver. Several aircraft transects on different days, partly without foehn, were made close to the scintillometer light paths. General characteristics of the foehn flow and turbulence implications for scintillometer measurements are discussed in sections 4a and 4b. Issues of scintillometer crosswind determination methods will be discussed in section 4c. Then the horizontal crosswind measurements will be compared with the lidar data and with aircraft measurements. Last, we compare the vertical crosswind measurements to aircraft data.

a. General characteristics of the scintillometer measurements

The 1-min-averaged measurements for 24 October 1999 are shown in Figs. 3 and 4. They exhibit a full cycle of foehn during its buildup (0000–0300 UTC), maturity (0300–1700 UTC), and subsequent decay (1700–2000 UTC) when a cold front moved into the area from the north. Table 3 contains basic statistics for the foehn phase, which was defined by requiring that the horizontal wind velocity was greater than 15 m s^{-1}. Horizontal crosswind speeds during this phase averaged 21 m s^{-1} for the Flusa scintillometer and 26 m s^{-1} at Ergellen. Both stations measured a strong downward component. Maximum vertical winds of $+3$ and -11 m s^{-1} were observed in the 1-min-averaged data; the average values of the vertical wind component during the foehn phase were -1.9 m s^{-1} for Flusa and -3.6 m s^{-1} for Ergellen.

b. Remarks on turbulence measurements

Although our scintillometers were not equipped for calibrated C_n^2 measurements, we can obtain qualitative information on the turbulence of the flow. This information is used to judge the performance of the scintillometer, especially under adverse conditions (fog or rain), when the instrument operation fails. Figure 5 shows the standard deviation of the light intensity for one channel of each scintillometer, which is proportional to C_n^2. From our experience, we consider values greater than about 200 to yield reliable wind measurements. This criterion was always fulfilled on that day. The maximum around 0300 UTC exhibits a reduced variability and occurred when the foehn air was eroding the top of the cold pool. This signal also shows a reduced variability in the high overall scintillation strength. We might hypothesize that water vapor from the cold-air pool in the valley is mixed upward into the foehn air. Together with the temperature distribution typical for a mixing process, this would produce density gradients relevant to scintillation. Then the reduced variability could be the signature of a homogeneous turbulence field with eddies of relatively small and mostly uniform size, as expected, for example, for Kelvin–Helmholtz waves. We do not have the means to test this hypothesis.

We further notice from Table 2 that the short-term fluctuations of the wind measurements vary by a factor of 2 for the whole day. The crosswind spectra for the foehn phase (wind speed >15 m s^{-1}) in Fig. 6 are nearly identical for both stations. The horizontal wind contains more energy than the vertical wind; hence the turbulence is not isotropic (Busch and Panofsky 1968). The spectra do not follow Kolmogorov theory, which predicts a $-5/3$ power drop-off in the inertial subrange. Our analysis technique is not very sensitive to changes of the turbulence spectrum (Wang et al. 1981). White noise appears for frequencies higher than 1 min^{-1}, mainly an effect of the large sampling volume (Andreas et al. 1992). The similarity of the spectra indicates that the turbulence characteristics of the foehn flow are very similar at both sites. From this we conclude that both instruments measure identically and that discrepancies between the measurements are real features of the flow, not of the instruments.

c. Comparison of crosswind measurement methods

Figure 7a shows a comparison of the slope method and the peak method with aircraft data for 14 transects with and without foehn. The 1-min averages of the scintillometers were compared with coincident aircraft measurements, as described above. The crosswind speeds were calculated with both methods from the same data. Apart from one outlier for the peak method, the linear regressions are very good, with variance R^2 values of about 0.9 (0.6 when the outlier was not removed). The regression equations indicate that there is a general tendency for the peak method to overestimate the wind speed for values less than 5 m s^{-1}, whereas the slope method overestimates the wind speed for values larger than about 10 m s^{-1} by about 20%. On the other hand, the peak method underestimates crosswind speeds by less than 10% for velocities between 15 and 30 m s^{-1}, and by less than 13% between 30 and 40 m s^{-1}. For all foehn phases between 20 and 24 October 1999, the ratio between slope and peak method measurements was close to 1.5 for Ergellen but much more variable for Flusa. Without independent measurements beyond the range of Fig. 7a we are not able to verify the exact wind speed.

The situation for the vertical velocities is different (Fig. 7b). Because they are generally less than a few meters per second, the slope method will deliver the

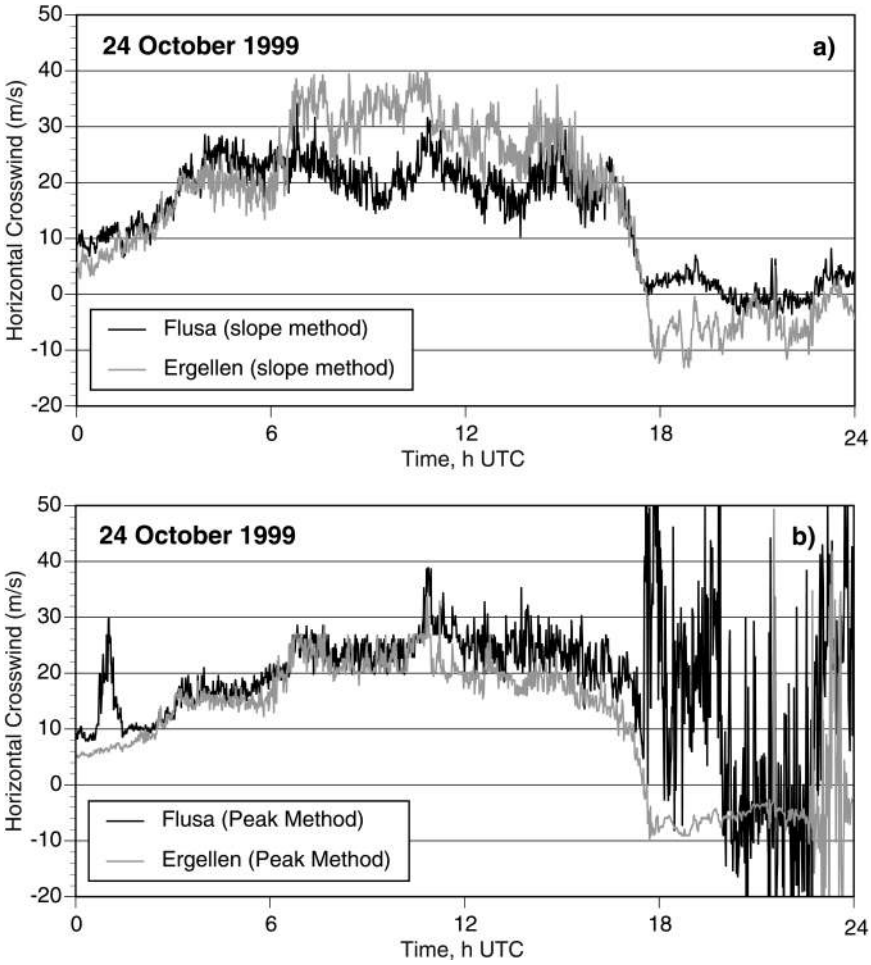

FIG. 3. The 1-min-averaged time series of horizontal crosswind measurements at Flusa and Ergellen for 24 Oct 1999, calculated with different techniques: (a) slope method and (b) peak method. Positive values indicate south-to-north flow.

better results. The regression yields a relative difference between scintillometer and aircraft measurements of 7%, but the scatter is large. Our data revealed that the peak method failed completely for vertical velocity measurements. One reason for this failure was the low maximum values of the covariance function that made a determination of the peak's position arbitrary. The foehn cases analyzed here showed maximum values of the normalized covariance function larger than 0.5, mostly around 0.8, for the horizontal component, but they were hardly larger than 0.4, and often less than 0.2, for the vertical component. These low values indicate that the scintillation signal is much less correlated for the vertical component than for the horizontal component, leading to a reduced signal-to-noise ratio (SNR) and thus to an increased measurement uncertainty. A strong decorrelation may change the calibration of the slope method toward an underestimation of the wind speed (Poggio 1998). The large vertical crosswind values we observed during foehn, however, indicate that this is probably not of concern here. The data scatter due to low SNR may be reduced with appropriate time averaging, for example, 10 min, or a 15-point running mean as indicated in Fig. 4b.

d. Validation of strong horizontal wind measurements

Figure 3a shows that the horizontal wind at Flusa determined by the slope method achieved speeds of 16–30 m s^{-1}, at which range it remained fairly constant during the whole foehn phase. Ergellen reveals more variations, especially the jump from 20 to 35 m s^{-1} at around 0630 UTC. This jump can be interpreted as the signature of a wind shift from south to southeast (Furger 2000). This shift would also mean that the foehn had to cross the Falknis mountain range (Fig. 2), which would provide a source for enhanced wave activity. This shift indeed coincides with the moment when the vertical velocity starts to deviate significantly from 0 at about 0700 UTC (Fig. 4). The peak method, on the other hand, does not reveal a substantial change between Flusa and Ergellen for the whole foehn phase (Fig. 3b). After

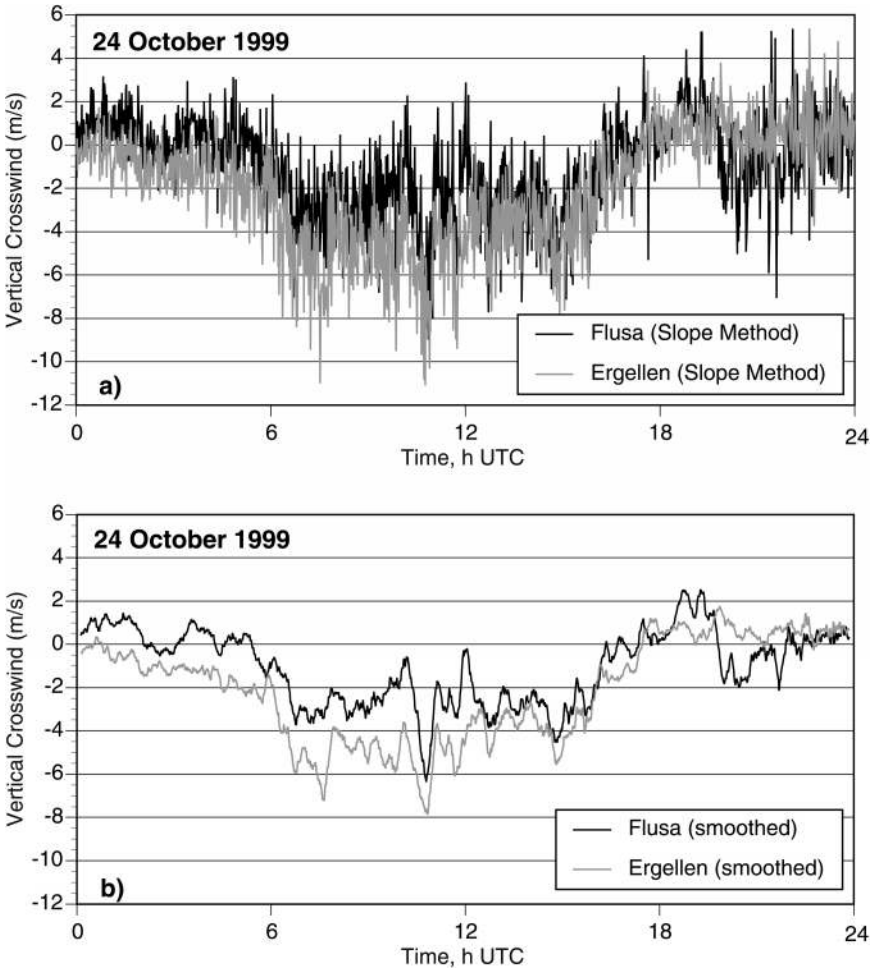

FIG. 4. The 1-min-averaged time series of vertical crosswind measurements obtained with the slope method at Flusa and Ergellen for 24 Oct 1999: (a) 1-min-averaged data and (b) 15-point running-average data. Positive values indicate upward flow.

foehn breakdown, peak measurements become very variable and unreliable. This behavior is typical for winds in the direction of the light paths, which illustrates one of the weaknesses of the peak method. Nevertheless, during the foehn phase the peak method matches the aircraft wind data better than the slope method does.

We used a lidar scan taken at 0937 UTC for our comparison (Table 4). At the lowest levels, most data were missing in the Sevelen area because the aerosol content of the foehn air was very low and did not produce enough backscatter intensity. We neglected projecting the radial wind component to the horizontal, because the correction is less than 2% for the lowest beam elevation angle. The difference in the orientation (azimuth angle) of the scintillometer beams and the different lidar azimuths would require another correction

TABLE 3. Characteristics of the foehn phase in the Rhine Valley during 24 Oct 1999, as derived from 1-min-averaged scintillometer data. Times are UTC.

Foehn Phase of 24 Oct 1999, 0230–1713 UTC (wind speed > 15 m s^{-1})		
	Flusa (slope method, m s^{-1})	Ergellen (slope method, m s^{-1})
Mean horizontal crosswind component	21.0	26.1
Std dev of horizontal crosswind component	3.8	6.9
Max horizontal crosswind component	34.3	40.2
Mean vertical crosswind component	−1.9	−3.6
Std dev of vertical crosswind component	2.1	2.2
Range of vertical crosswind component	−9.0 to 3.1	−11.1 to 1.4

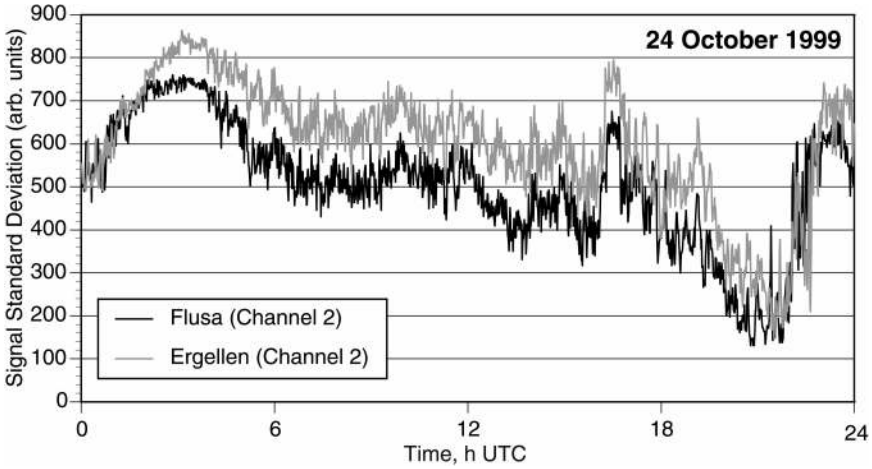

FIG. 5. Standard deviations of signal strength in arbitrary units for channel 2 at Flusa and Ergellen for 24 Oct 1999.

that depends on the mean flow direction. The angle between the Flusa crosswind component and the lidar wind component is in the range between $-15°$ and $+5°$. The Ergellen crosswind direction deviates between 30° and 60° from the lidar beam direction. Because the data in the vicinity of the scintillometers were too sparse for a point-by-point intercomparison, we also neglected the azimuth correction. The area average over all measured radial velocities in the circular arc was 19.4 m s^{-1} at 4° elevation. Average lidar values close to the scintillometer beams (the numbers printed in boldface type in Table 4) were 17.1 m s^{-1} for Flusa and 18.2 m s^{-1} for Ergellen. Velocities at individual range gates ranged from 0.8 to 46.7 m s^{-1} (italic numbers in Table 4). These values indicate that the wind field was inhomogeneous and that extreme velocities were confined to very localized areas. The scintillometers measured 16.5 m s^{-1} at Flusa and 33.5 m s^{-1} at Ergellen with the slope method during the corresponding 5-min interval. It is not yet clear why this discrepancy occurred with the slope method. The peak method, at the same time, yielded 24.0 and 24.5 m s^{-1}, respectively. Because this was the only scan available at scintillometer height for that foehn phase, we could not reduce the scatter in the data by averaging.

Statistics of aircraft wind measurements for 24 October 1999 are given in Table 5, in which an increase in wind speed with decreasing altitude becomes manifest. It is well known that foehn flows exhibit maximum wind speeds at low altitudes, that is, within the valleys. We may expect that the value of 26 m s^{-1} is typical also for the scintillometer height, where it compares well with the horizontal measurements.

e. Validation of vertical velocity measurements

The vertical crosswind component in Fig. 4 shows that both scintillometers measure similar vertical winds that vary with similar amplitudes and phases. Until foehn breakdown at 1700 UTC, Flusa vertical winds were generally less negative than Ergellen winds. Then, after about 2000 UTC, the situation reversed. We conclude again that there is no systematic difference between the instruments and that the differences may be attributed to inhomogeneities of the wind field.

The aircraft encountered significant wave activity and turbulence during its flight along the Rhine valley. Vertical velocities in the range between -3 and $+4$ m s^{-1} (1-min averages) or -8 and $+10$ m s^{-1} (1-Hz samples) were observed. The best-developed examples of waves were encountered at 1430 and 1600 m above mean sea level (MSL; Fig. 8a), at which heights horizontal wind speeds dropped to one-half within a 1-km distance. This happened directly above the scintillometers and was observed in both aircraft trajectories, separated by more than an hour. This observation indicates that the wave in this area was stationary but also that flow dynamics played a crucial role here and horizontal homogeneity of the wind field was not established. The aircraft vertical velocities (Fig. 8b) varied in the same range of values as those of the scintillometers. Their standard deviations were of the same order of magnitude (Table 5). In contrast to the scintillometer measurements, the aircraft vertical winds were not systematically negative close to the scintillometers. We attribute this to spatial and temporal variations of the vertical velocity field, and support our scintillometer values by the average vertical velocities for the 10-km transects centered around Sevelen, -0.22 m s^{-1} for 1600 m MSL and -0.10 m s^{-1} for 1430 m MSL, which indicate a general downward motion in the larger area (Table 5). As shown in Fig. 7, the correlation between aircraft and scintillometer vertical winds for all cases is positive, which further corroborates our findings. Figure 9 shows scatter diagrams of the vertical versus the horizontal crosswind components averaged over 10 min. Each dot marks the

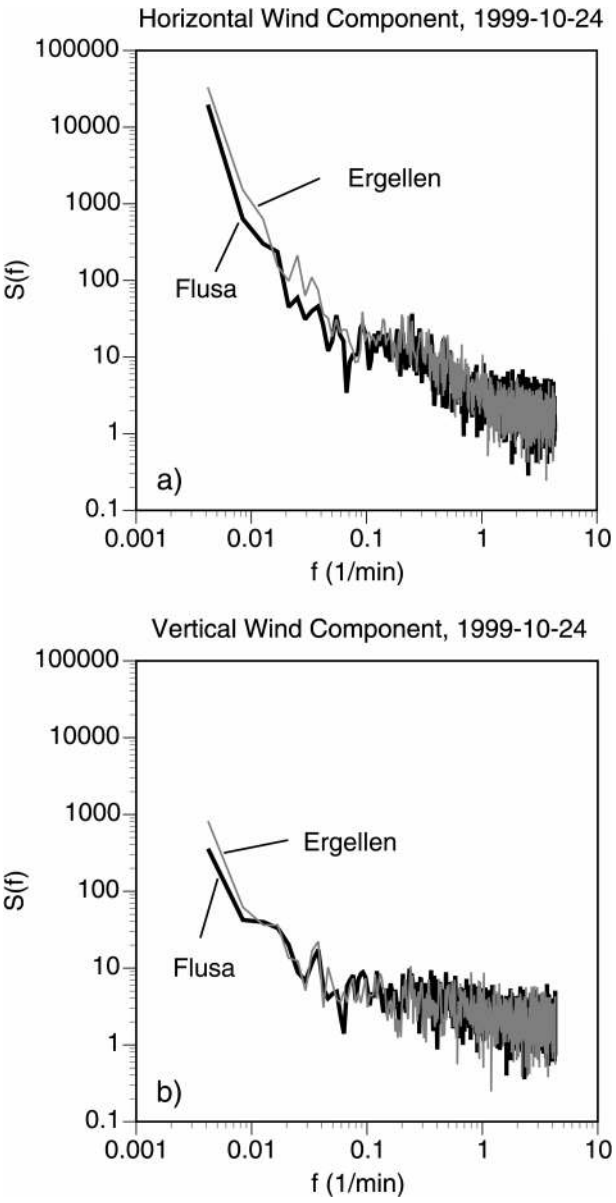

FIG. 6. Crosswind power spectra for 24 Oct 1999: (a) horizontal component and (b) vertical component.

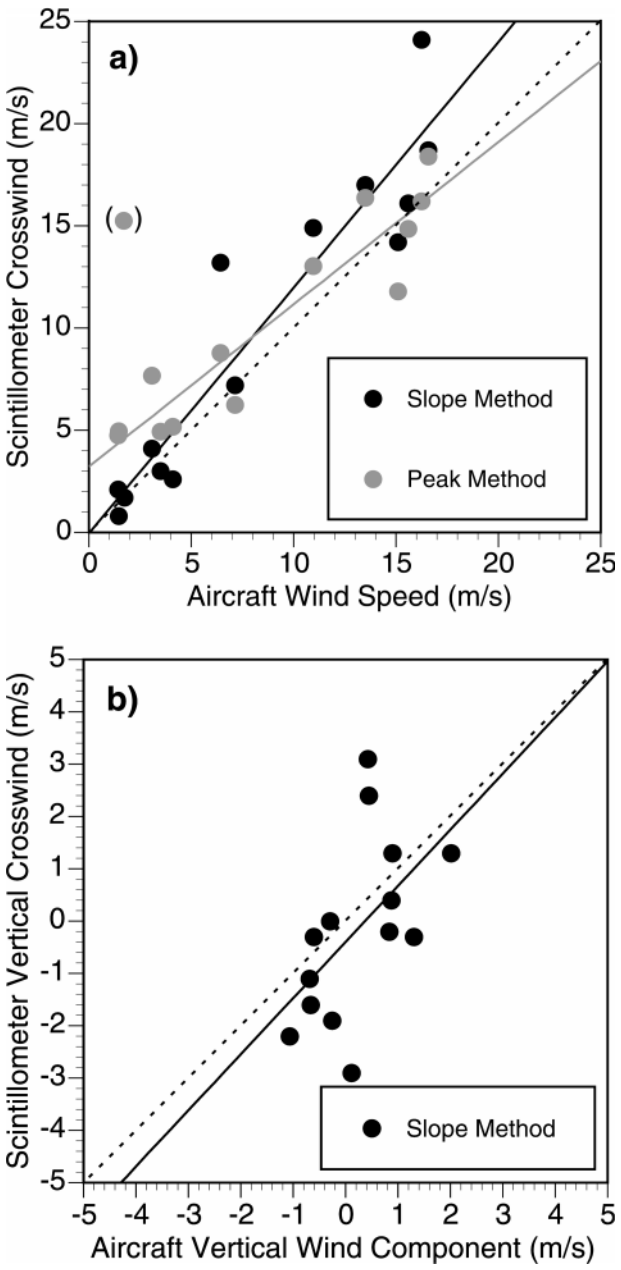

FIG. 7. Scatterplot of (a) scintillometer horizontal crosswind vs aircraft horizontal wind speed and (b) scintillometer vertical crosswind vs aircraft vertical wind component. Scintillometer data are 1-min averages. Aircraft data were averaged over a flight transect centered at the scintillometer light path extending about 200 m on either side. Data were taken from flights on 20–22 Oct 1999. The outlier in brackets in (a) was not considered for the regression analysis. Horizontal wind regression equations are $v_s = 1.20\text{ff} - 0.05$ for the slope method and $v_s = 0.79\text{ff} + 3.21$ for the peak method, v_s being the scintillometer crosswind speed and ff the aircraft wind velocity. The vertical wind regression equation is $w_s = 1.07\ \text{ff} - 0.40$, with w_s being the scintillometer vertical crosswind.

end point of a vector starting at the coordinate origin. Horizontal and vertical wind components were strongly correlated with each other at Ergellen (Fig. 9a), with a correlation coefficient $r = -0.93$ but were less so for Flusa (Fig. 9b), for which $r = -0.54$. The correlation for shorter averaging intervals was smaller, indicating local effects of turbulence. The ratio between the vertical and the horizontal component is the tangent of the angle of the incident flow. The 1-min-average angle during foehn was $-7.4° \pm 3.6°$ for Ergellen and $-5.1° \pm 5.5°$ for Flusa, which is between the angle of the almost horizontal valley floor and the angle of a straight line to the Falknis mountain upstream in the southeast

TABLE 4. Radial velocity measurements (m s^{-1}) obtained with the French TWL at 0937 UTC on 24 Oct 1999 for different distances from the lidar (km). Beam elevation was 4°. The header lists the azimuth angle of lidar beam. Blank cells indicate unreliable data [see Dabas et al. (1999) for quality control procedure]. See Fig. 2 for geographical information. Measurements close to the light paths are printed in boldface, with the Ergellen path along the diagonal of the table. Max and min values are in italics. Corresponding scintillometer measurements were 16.5 m s^{-1} in Flusa (horizontal row at the bottom of the table) and 33.5 m s^{-1} in Ergellen (diagonal of the table).

Distance (km)	Azimuth (°)						
	3	8	13	18	23	28	33
7.13		26.7	14.8	17.0	23.3		14.1
7.50	**13.0**	19.0	15.8	6.7	1.4		17.2
7.88			22.6	19.8	*46.7*		
8.25	18.7	**22.0**	29.9		10.6		21.6
8.63		**25.2**	**15.8**	21.1	23.8		
9.00	17.1		**18.3**		3.7		
9.38	15.9	15.9	**22.1**		17.2		28.0
9.75			19.0				38.7
10.13			−11.1		**10.4**		31.9
10.50		30.9	19.4				
10.88		16.1	12.0		**26.2**		
11.25							
11.63				24.0			
12.00			**38.5**		7.9		
12.38		**25.7**			**11.3**		***0.8***
12.75	22.3				**14.4**		**1.1**
13.13						6.6	

(approximately 13°). If the calibration were incorrect, the average angle would not change; that is, we would not detect a calibration error by comparing the two flow components. Direct vertical wind comparisons with the lidar were not yet possible for the Sevelen area, because reduced backscatter in the aerosol-poor foehn air meant too many data points were missing at this range from the lidar for a composition of range–height indicator scans. However, data obtained with a velocity–azimuth display technique directly above the lidar in Vilters also exhibited values in the range between −5 and +5 m s^{-1} for the vertical velocity. Using the regression from the vertical and horizontal components of the scintillometers, we estimate the lidar vertical wind components in the Sevelen column to be about −3 m s^{-1} (beam average), with a maximum value of −6.8 m s^{-1}.

5. Conclusions

We have presented direct measurements of the horizontal and vertical crosswind components obtained with large-aperture scintillometers located some 500 m above ground in an alpine valley during strong foehn conditions. We used three-mirror instruments to measure the horizontal and vertical crosswind components simultaneously. Based on the power spectra, we showed that both instruments worked identically and that differences in the measurements must be attributed to the flow, not the instruments.

We compared the slope method and the peak technique for the determination of the crosswind with each other and with aircraft measurements. They showed systematic differences. In the strong wind regime, the slope method tended to overestimate the wind speed by 20%, whereas the peak technique underestimated the wind speed by 13% at most. These estimates are still coarse because of the small number of measurements analyzed, and further measurements are needed to adjust these uncertainties. Vertical velocities could only be measured with the slope method. The poor SNR required sufficient averaging times to reduce the noise. Our results also illustrate the difficulty in selecting the appropriate method for the determination of crosswind speeds. Although the peak method showed smaller deviations from the

TABLE 5. Statistics of 1-s aircraft data for three 10-km transects (216–226 km north in Swiss coordinates) at Sevelen, 24 Oct 1999. The 1-min scintillometer data for comparison are given in the bottom row.

	Mean	Std dev	Mean	Std dev	Mean	Std dev
Altitude (m MSL)	1371		1434		1602	
Horizontal wind speed (m s^{-1})	26.1	2.12	22.3	3.69	22.4	2.53
Vertical wind component (m s^{-1})	−0.71	1.80	−0.10	2.42	−0.22	2.30
Flusa scintillometer vertical wind component (m s^{-1})	−2.02	3.61	−0.55	1.49	−2.86	2.35
Ergellen scintillometer vertical wind component (m s^{-1})	−6.02	2.15	−3.97	1.30	−5.12	0.80

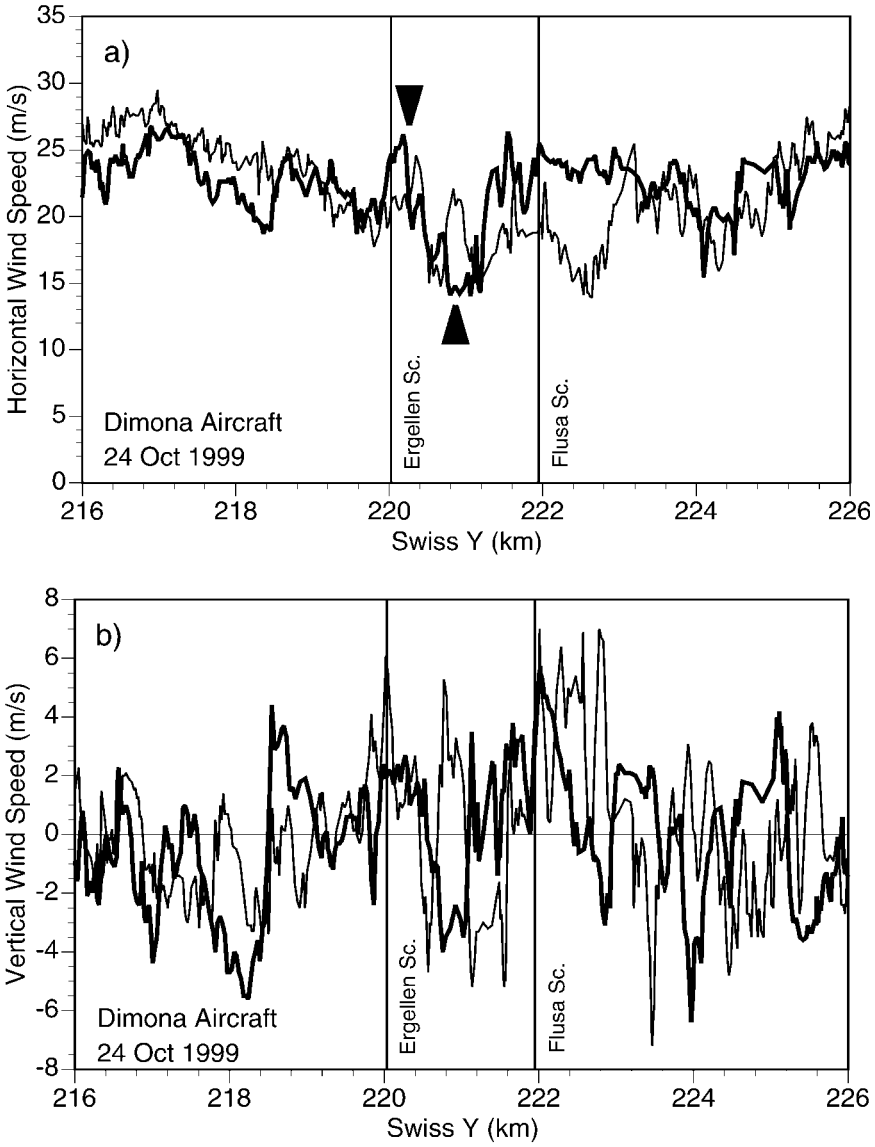

FIG. 8. Aircraft measurements (1 Hz) of (a) horizontal and (b) vertical wind speed above Sevelen for 24 Oct 1999: (thick line) 0900–0906 UTC, mean altitude 1600 m MSL and (thin line) 1011–1018 UTC, mean altitude 1430 m MSL. The black arrows indicate the velocity drop mentioned in the text.

aircraft measurements for the horizontal component, it failed completely for the vertical component. Hence we consider the slope method to be superior because of its consistency for both components and its better accuracy for lower wind speeds. This result is in contrast to earlier findings of Poggio et al. (2000) but is in good agreement with Wang et al. (1981).

Intercomparisons of the horizontal wind component with lidar data and of the horizontal and vertical components with aircraft data showed that both vertical and horizontal wind field characteristics were reproduced well, even during phases of strong winds. The vertical crosswind velocities exhibited the same variability as did the aircraft measurements. Differences among lidar, aircraft, and scintillometer measurements were attributed to dynamic and topographic effects not accounted for by the simple analysis techniques. The uncertainties remained within the estimated uncertainty of the crosswind measurements. We thus consider the measurements of the horizontal and vertical crosswind components to be valid. The feasibility of meaningful vertical velocity measurements with scintillometers has been demonstrated.

Our results show that scintillometry is another method to obtain horizontal and vertical wind measurements at elevated layers in valleys. Crosswind scintillometers

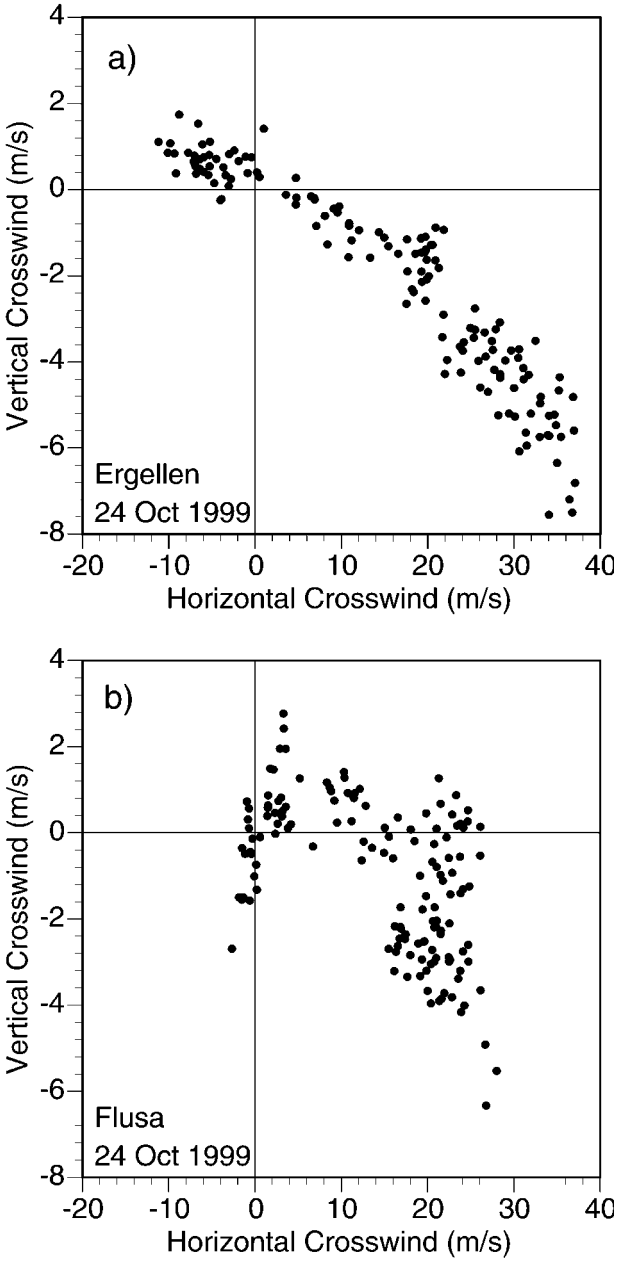

FIG. 9. Scatterplot of vertical vs horizontal crosswind components at (a) Ergellen and (b) Flusa for 24 Oct 1999. Positive horizontal crosswinds indicate southerly flow (foehn); negative vertical crosswinds indicate downward motion.

are relatively low in cost and are easy to operate continuously with a high temporal resolution. They are suited well for wind monitoring applications. Our method yields interesting results in complex terrain, over which significant vertical air motions can occur.

A natural next step will be the study of dynamical aspects of foehn flows. The scintillometer data collected during MAP–FORM contain interesting information on vertical motion within valleys during foehn. The data also offer the prospect for studying the dynamics of foehn-induced waves, especially the energetics of gravity waves. Other case studies may reveal more on the local inhomogeneity and unstationarity of foehn flows.

Acknowledgments. Our thanks go to Robert Erne, René Richter, Remo Nessler, and Gérard Stefanicki for technical help in the field and to Michel Tinguely for programming assistance. Willi Fuchs piloted the aircraft. We are grateful to the farmer families in Ergellen and Flusa and to the community of Triesenberg, Liechtenstein, for their interest and support.

REFERENCES

Andreas, E. L, J. R. Gosz, and C. N. Dahm, 1992: Can long-path FTIR spectroscopy yield gas flux measurements through a variance technique? *Atmos. Environ.*, **26A,** 225–233.

Bougeault, P., and Coauthors, 2001: The MAP special observing period. *Bull. Amer. Meteor. Soc.*, **82,** 433–462.

Brinkmann, W. A. R., 1971: What is foehn? *Weather,* **26,** 230–239.

Busch, N. E., and H. A. Panofsky, 1968: Recent spectra of atmospheric turbulence. *Quart. J. Roy. Meteor. Soc.,* **94,** 132–148.

Clifford, S. F., G. R. Ochs, and R. S. Lawrence, 1974: Saturation of optical scintillation by strong turbulence. *J. Opt. Soc. Amer.*, **64,** 148–154.

Dabas, A. M., P. Drobinski, and P. H. Flamant, 1999: Adaptive filters for frequency estimates of heterodyne Doppler lidar returns: Recursive implementation and quality control. *J. Atmos. Oceanic Technol.*, **16,** 361–372.

Doviak, R. J., and D. S. Zrnić, 1993: *Doppler Radar and Weather Observations.* 2d ed. Academic Press, 562 pp.

Drobinski, P., R. A. Brown, P. H. Flamant, and J. Pelon, 1998: Evidence of organized large eddies by ground-based Doppler lidar, sonic anemometer and sodar. *Bound.-Layer Meteor.*, **88,** 343–361.

——, A. M. Dabas, P. Delville, P. H. Flamant, J. Pelon, and R. M. Hardesty, 1999: Refractive-index structure parameter in the planetary boundary layer: Comparison of measurements taken by a 10.6 μm-coherent lidar, a 0.9 μm-scintillometer, and in-situ sensors. *Appl. Opt.*, **38,** 1648–1656.

——, ——, C. Haeberli, and P. H. Flamant, 2001: On the small-scale dynamics of flow splitting in the Rhine valley during a shallow foehn event. *Bound.-Layer Meteor.*, **99,** 277–296.

Furger, M., 2000: Crosswind measurements with scintillometers at 500 m above valley floor during foehn. Preprints, *Ninth Conf. on Mountain Meteorology*, Aspen, CO, Amer. Meteor. Soc., 75–78.

——, and Coauthors, 2000: The VOTALP Mesolcina Valley Campaign 1996—concept, background and some highlights. *Atmos. Environ.*, **34,** 1395–1412.

Hill, R. J., S. F. Clifford, and R. S. Lawrence, 1980: Refractive-index and absorption fluctuations in the infrared caused by temperature, humidity and pressure fluctuations. *J. Opt. Soc. Amer.*, **70,** 1192–1205.

——, G. R. Ochs, J. J. Wilson, D. A. Furtney, and J. T. Priestley, 1991: Results of the 1988 fluxes-from-scintillation experiment. NOAA Tech. Memo. ERL-WPL-192, 147 pp.

Hoinka, K. P., 1985: Observation of the airflow over the Alps during a foehn event. *Quart. J. Roy. Meteor. Soc.*, **111,** 199–224.

Kohsiek, W., 1985: A comparison between line-averaged observation of C_n^2 from scintillation of a CO_2 laser beam and time-averaged in-situ observations. *J. Climate Appl. Meteor.*, **24,** 1099–1103.

Lawrence, R. S., G. R. Ochs, and S. F. Clifford, 1972: Use of scintillations to measure average wind across a light beam. *Appl. Opt.*, **11,** 239–243.

Lee, R. W., and J. C. Harp, 1969: Weak scattering in random media, with applications to remote sensing. *Proc. IEEE,* **57,** 375–406.

Neininger, B., W. Fuchs, M. Baeumle, A. Volz-Thomas, A. S. H. Prévôt, and J. Dommen, 2001: A small aircraft for more than just ozone: MetAir's ''Dimona'' after ten years of evolving development. Preprints, *11th Symp. on Meteorological Observations and Instrumentation*, Albuquerque, NM, Amer. Meteor. Soc., 123–128.

Pettré, P., 1982: On the problem of violent valley winds. *J. Atmos. Sci.*, **39,** 542–554.

Poggio, L., 1998: Use of scintillation measurements to determine fluxes in complex terrain. Abteilung für Umweltnaturwissenschaften, Eidgenössische Technische Hochschule, Diss. ETH No. 12755, 148 pp.

——, M. Furger, A. S. H. Prévôt, W. K. Graber, and E. L Andreas, 2000: Scintillometer wind measurements over complex terrain. *J. Atmos. Oceanic Technol.,* **17,** 17–26.

Press, W. H., B. P. Flannery, S. A. Teukolsky, and W. T. Vetterling, 1989: *Numerical Recipes: The Art of Scientific Computing (FORTRAN Version).* Cambridge University Press, 702 pp.

Seibert, P., 1990: South foehn studies since the ALPEX experiment. *Meteor. Atmos. Phys.*, **43,** 91–103.

Wang, T., G. R. Ochs, and S. F. Clifford, 1978: A saturation-resistant optical scintillometer to measure C_n^2. *J. Opt. Soc. Amer.*, **68,** 334–338.

——, ——, and R. S. Lawrence, 1981: Wind measurements by the temporal cross-correlation of the optical scintillations. *Appl. Opt.*, **20,** 4073–4081.

Willis, G. E., and J. W. Deardorff, 1976: On the use of Taylor's translation hypothesis for diffusion in the mixed layer. *Quart. J. Roy. Meteor. Soc.*, **102,** 817–822.